

Direct Measurement of the Bose-Einstein Condensation Universality Class in $\text{NiCl}_2\text{-4SC}(\text{NH}_2)_2$ at Ultralow Temperatures

L. Yin,¹ J. S. Xia,¹ V. S. Zapf,² N. S. Sullivan,¹ and A. Paduan-Filho³

¹*Department of Physics, University of Florida, and National High Magnetic Field Laboratory, Gainesville, Florida 32611-8440, USA*

²*National High Magnetic Field Laboratory, Los Alamos National Laboratory, MS E-536, Los Alamos, New Mexico 87545, USA*

³*Instituto de Física, Universidade de São Paulo, Caixa Postal 66.318, 05315-970, São Paulo, Brazil*
(Received 19 July 2008; revised manuscript received 5 September 2008; published 31 October 2008)

In this work, we demonstrate field-induced Bose-Einstein condensation (BEC) in the organic compound $\text{NiCl}_2\text{-4SC}(\text{NH}_2)_2$ using ac susceptibility measurements down to 1 mK. The Ni $S = 1$ spins exhibit 3D XY antiferromagnetism between a lower critical field $H_{c1} \sim 2$ T and an upper critical field $H_{c2} \sim 12$ T. The results show a power-law temperature dependence of the phase transition line $H_{c1}(T) - H_{c1}(0) = aT^\alpha$ with $\alpha = 1.47 \pm 0.10$ and $H_{c1}(0) = 2.053$ T, consistent with the 3D BEC universality class. Near H_{c2} , a kink was found in the phase boundary at approximately 150 mK.

DOI: [10.1103/PhysRevLett.101.187205](https://doi.org/10.1103/PhysRevLett.101.187205)

PACS numbers: 75.40.-s, 65.40.Ba

The idea of Bose-Einstein condensation (BEC) occurring in the spin systems of certain quantum magnets with axial symmetry has been explored extensively in the past few years [1]. The idea was suggested by Affleck [2] and worked out in detail for 3D spin ladder systems by Giamarchi and Tsvelik [3]. Early investigations of BEC in the compound TlCuCl_3 [4] generated a flurry of interest in this field, although BEC in that compound was later called into question in an oft-overlooked electron spin resonance (ESR) study [5]. Many new candidate BEC systems have since been proposed including $\text{BaCuSi}_2\text{O}_6$, Cs_2CuCl_4 , and $\text{NiCl}_2\text{-4SC}(\text{NH}_2)_2$ [6–16].

In these compounds, the axial symmetry of the spins allows XY antiferromagnetic order to occur over certain ranges of temperature and magnetic field. Near the critical magnetic fields where the long-range order is induced or suppressed, the spin system can be mapped onto a system of dilute hard-core bosons on a lattice and the field-induced quantum phase transition at the boundary of the long-range ordered state can be modeled as a Bose-Einstein condensation [3,17–20]. The caveat is that in quantum magnets the boson number is proportional to the longitudinal magnetization, and thus is conserved in equilibrium rather than strictly on all time scales. Therefore, in quantum magnets only the *thermodynamic properties* of the system should follow the predictions of BEC theory and nonequilibrium effects such as supercurrents will not occur. Nevertheless, these compounds provide an important test of BEC phase transition in the thermodynamic limit.

A key experimental signature of BEC is a power-law temperature-dependence of the critical field line $H_c - H_c(0) \propto T^\alpha$ where $\alpha = 3/2$ [21,22]. This power-law corresponds to the low-temperature limit of the boson distribution function. It is important to note that this power-law is valid in the limit of very low temperatures. So far very

few quantum magnet BEC candidate have been studied at temperatures well below the energy scales for boson interactions, which are given by the antiferromagnetic couplings between spins. Furthermore, if the temperature range at which the power-law fit is performed is far from zero temperature, then it is very difficult to accurately identify the intercept, and the resulting power-law exponent that is derived from the fit is highly dependent on the value of the intercept used [10]. One way to circumvent this problem is the windowing method in which the intercept and the exponent are determined more-or-less independently by performing fits over different temperature ranges and extrapolating the values of the intercept and the exponent to zero temperature [23]. However, this extrapolation technique from higher temperatures does not always correspond to the actual low-temperature behavior. This was seen in the compound $\text{BaCuSi}_2\text{O}_6$, where at temperatures above 1 K, the windowing method yields one exponent, but due to a reduction in dimensionality of the spin system, a different exponent can be observed at lower temperatures [24].

Here we report a direct observation of the $3/2$ power-law exponent of the 3D BEC universality class at ultralow temperatures in the compound dichloro tetrakis-thiourea nickel (DTN) with chemical formula $\text{NiCl}_2\text{-4SC}(\text{NH}_2)_2$. Our measurements were performed at temperatures down to 1 mK, which is 2 orders of magnitude below the lowest temperature scale for magnetic coupling in this system $J_a = 180$ mK, and the lowest temperature ever used to investigate BEC in a quantum magnet. Thus we do not have to use any extrapolation to determine the power-law exponent.

The organic magnet DTN contains $S = 1$ Ni^{2+} atoms that form two interpenetrating tetragonal lattices. At zero field, a uniaxial anisotropy $D \sim 9$ K splits the Ni $S = 1$

triplet into a $S_z = 0$ ground state and a $S_z = \pm 1$ excited doublet. The $S_z = 1$ state can be suppressed with applied magnetic fields along the tetragonal c -axis via the Zeeman effect, thus producing a magnetic ground state above $H_{c1} = 2.1$ T. Antiferromagnetic coupling between the Ni atoms with exchange strength $J_c = 2.2$ K along the c axis and $J_a = 0.18$ K perpendicular to the c axis produces long-range antiferromagnetic order [25]. The long-range order occurs in a dome-shaped region of the T - H phase diagram between H_{c1} , where the magnetic ground state is induced, and H_{c2} where the spins align with the applied magnetic field and below $T = 1$ K [12]. The XY symmetry, the magnetic exchange couplings and the uniaxial anisotropy D have been identified via inelastic neutron scattering and electron spin resonance (ESR) [12,25]. The power-law dependence of the critical field line H_{c1} was previously investigated using specific heat and magnetocaloric effect measurements down to a minimum temperature of 100 mK [12] using the windowing method, and a power law consistent with $\alpha = 3/2$ was determined. This power law was also investigated using magnetization measurements to 0.5 K [26]. The validity of this power law was called into question, however, due to the fact that it is an extrapolation rather a direct measurement, in particular, in light of the recent new results for $\text{BaCuSi}_2\text{O}_6$ showing a different exponent at low temperatures [24].

We have now measured the power-law temperature dependence of the critical field H_{c1} down to 1 mK using ac susceptibility. The experiments were carried out using a PrNi_5 nuclear refrigerator and a 15 T magnet at the High B/T facility of National High Magnetic Field Laboratory. The sample was immersed in liquid ^3He in a polycarbonate cell, and thermal contact to the refrigerator was assured via sintered silver that was an integral part of an assembly of annealed silver rods extending from the nuclear refrigerator. The temperature was calibrated using a ^3He melting-pressure curve thermometer mounted in the zero-field region of the magnet at the top of the nuclear stage. Both ac and dc magnetic fields were applied in the direction parallel to the c axis of the single crystal of DTN. An ac signal with an amplitude between 0.5 and 1 G and a low frequency of 275 Hz was generated in a primary coil wound from superconducting NbTi wire, thereby avoiding heating at ultralow temperatures. The ac susceptibility χ_{ac} was measured by sweeping the external dc field at rates between 0.1 and ~ 0.001 T/min while the temperature was fixed at various values between 270 and 1.0 mK.

Figure 1 shows three traces of ac susceptibility χ_{ac} for temperatures of 20, 150, and 600 mK spanning the entire magnetic field region, with a relatively fast sweep rate of 0.054 T/min. The typical field-induced long-range AFM (BEC) transitions appears as steps in these traces with $H_{c1} \sim 2$ T and $H_{c2} \sim 12$ T. As the temperature is lowered, the steps become sharper and a peak develops near H_{c2} .

The values of H_{c1} and H_{c2} were determined from field sweeps over smaller field ranges at 0.0068 T/min. The

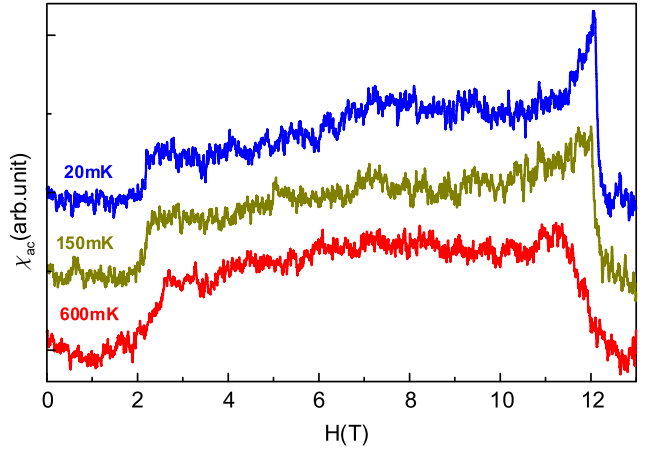


FIG. 1 (color online). ac susceptibility, χ_{ac} , as a function of magnetic field H with a field sweep rate of 0.054 T/min. Traces are shown for $T = 20$ mK (the highest curve), 150 and 600 mK.

peak in the first derivative of the ac susceptibility $d\chi_{ac}/dH$ was used to identify H_{c1} and H_{c2} , as shown in Fig. 2. We measured each field sweep at a given temperature 4 to 5 times. Then, since this did not produce enough statistics to determine an accurate error bar for each individual data point, we averaged all of the error bars to produce a single uniform error bar. This is a reasonable approach since the noise in the field sweeps and the resulting error bars were roughly the same from low temperatures to high temperatures. In the critical field—temperature phase diagram shown in Figs. 3(a) and 3(b), the temperature dependence of H_{c1} and H_{c2} have been plotted separately. As shown in Fig. 3(a), H_{c2} saturates at 12.175 T as T approaches zero.

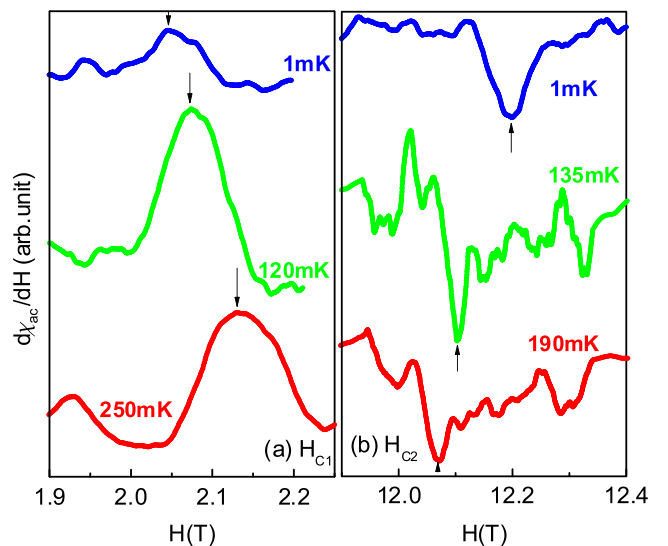


FIG. 2 (color online). The first derivative of the ac susceptibility $d\chi_{ac}/dH$ for H_{c1} [Fig. 2(a)] and H_{c2} [Fig. 2(b)], respectively, with a field sweep rate of 0.0068 T/min. The arrows indicate the peaks, which were identified as the critical values of H_{c1} and H_{c2} .

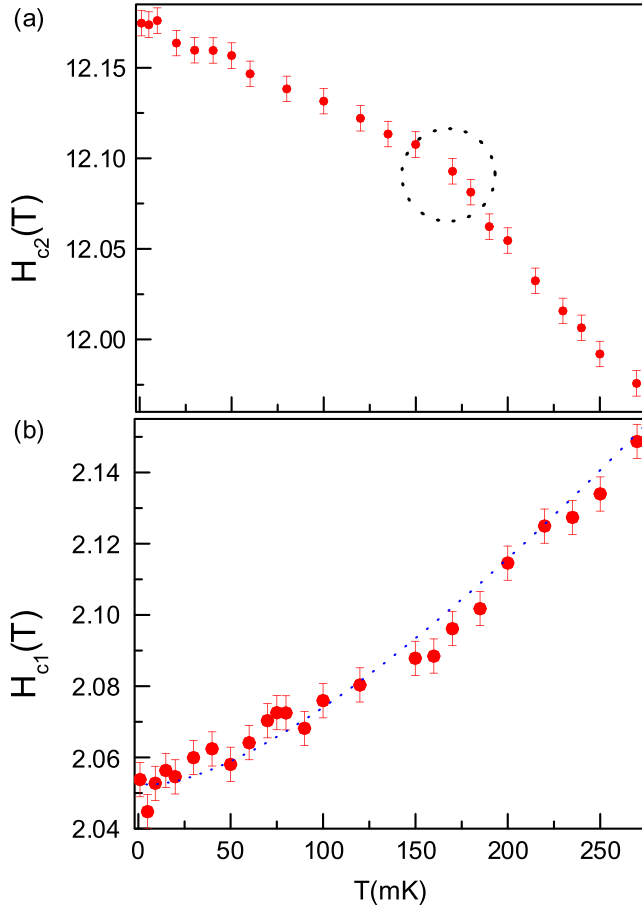


FIG. 3 (color online). (a) The temperature dependence of the upper critical field H_{c2} for a field sweep rate of 0.0068 T/min. The dashed circle shows an abnormal change in slope. (b) The temperature dependence of the lower critical field H_{c1} in a field sweep rate of 0.0068 T/min. The line is a fit to the equation $H_{c1}(T) - H_{c1}(0) \sim T^\alpha$ with $\alpha = 1.47 \pm 0.10$ and $H_{c1}(0) = 2.053$ T.

However, there exists a region marked by a dashed circle at approximately 150 mK, where a shoulder appears. The origin of this anomaly is unclear at this point.

For H_{c1} in Fig. 3(b), we fit a power-law temperature dependence $H_{c1}(T) - H_{c1}(0) = aT^\alpha$ to the data between 1 and 260 mK, yielding an intercept of 2.053 T and an exponent of 1.47 ± 0.10 as shown in Fig. 1. In order to demonstrate that the exponent is robust and independent of the intercept, we also performed fits to the data with the intercept held fixed for various intercepts between 2.04 and 2.06 T in Fig. 4. The table in the figure indicates the exponent, its error bar, and the value of χ^2 for each fit. The intercept with the lowest value of χ^2 is $H_{c1}(0) = 2.053$ T, yielding an exponent α of 1.46 in that fit. Furthermore, all the fits for all the intercepts yield values close to 1.5. Finally we show H_{c1} as a function of $T^{1.5}$ in Fig. 5. The inset shows the same data as a function of T^2 , showing that we can rule out that temperature dependence.

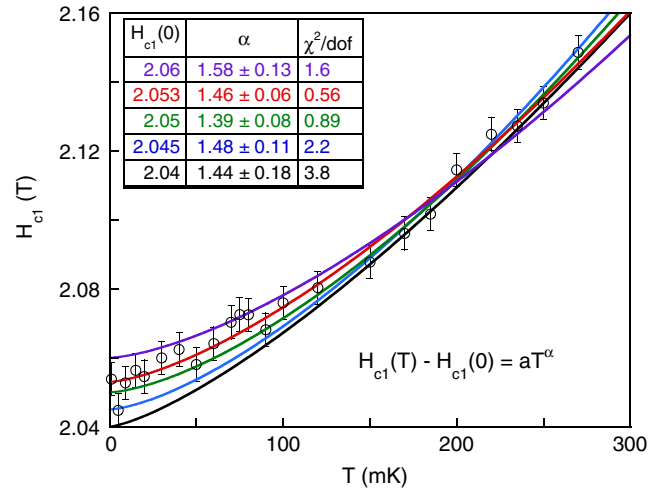


FIG. 4 (color online). (a) The critical field H_{c1} as a function of temperature T . The lines are fits of the equation $H_{c1}(T) - H_{c1}(0) = aT^\alpha$, where $H_{c1}(0)$ is held fixed and a and α are allowed to vary.

Thus, the best fit yields an exponent $\alpha = 1.47 \pm 0.10$, which closely matches the expected exponent $\alpha = 1.5$ for a quantum phase transition in the 3D BEC universality class. Other nearby universality classes such as the 3D Ising ($\alpha = 2$) and 2D BEC ($\alpha = 1$) can be excluded.

In conclusion, we have established that the field-induced quantum phase transition at H_{c1} in DTN belongs to the 3D BEC universality class by directly measuring the power-law exponent in the relation $H_{c1}(T) - H_{c1}(0) \propto T^\alpha$ down to 1 mK. This is the first example of a direct measurement of this exponent at temperatures far below the energy scales for antiferromagnetic coupling in a magnetic insulator.

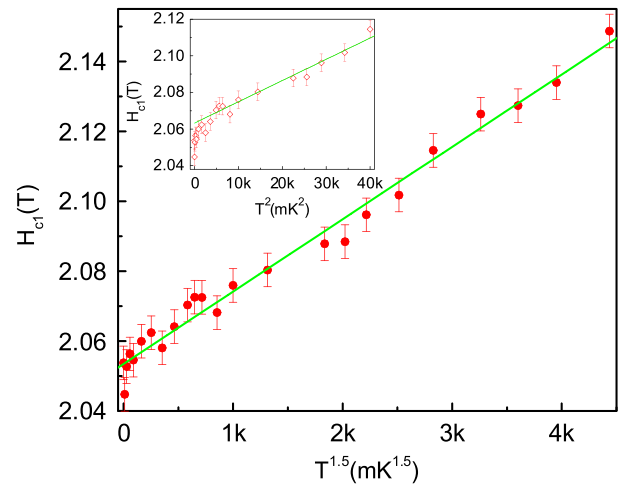


FIG. 5 (color online). The lower critical field H_{c1} as a function of T^α , where $\alpha \sim 1.5$. The dashed straight line is the linear fit to this trace. Inset: H_{c1} as a function of T^α , where $\alpha \sim 2$.

These measurements were carried out at the High B/T facility of the National High Magnetic Field Laboratory and were supported by the National Science Foundation Cooperative Agreement No. DMR 0654118, the Department of Energy and the State of Florida. A. P. F. acknowledges support from the Brazilian Agencies CNPq and FAPESP.

-
- [1] T. Giamarchi, C. Rüegg, and O. Tchernyshyov, *Nature Phys.* **4**, 198 (2008).
- [2] I. Affleck, *Phys. Rev. B* **43**, 3215 (1991); *ibid.* **43**, 3215 (1991).
- [3] T. Giamarchi and A. M. Tsvelik, *Phys. Rev. B* **59**, 11 398 (1999).
- [4] C. Rüegg, N. Cavadini, A. Furrer, H.-U. Güdel, K. Krämer, H. Mutka, A. Wildes, K. Habicht, and P. Vorderwisch, *Nature (London)* **423**, 62 (2003).
- [5] V. N. Glazkov, A. I. Smirnov, H. Tanaka, and A. Oosawa, *Phys. Rev. B* **69**, 184410 (2004).
- [6] M. Jaime *et al.*, *Phys. Rev. Lett.* **93**, 087203 (2004).
- [7] A. Paduan-Filho, X. Gratens, and N. F. Oliveira Jr., *Phys. Rev. B* **69**, 020405(R) (2004).
- [8] T. Waki, Y. Morimoto, M. Kato, K. Yoshimura, H. Mitamura, and T. Goto, *Physica (Amsterdam)* **359–361B**, 1372 (2005).
- [9] T. Radu, H. Wilhelm, V. Yushankhai, D. Kovrizhin, R. Coldea, Z. Tylczynski, T. Lühmann, and F. Steglich, *Phys. Rev. Lett.* **95**, 127202 (2005).
- [10] S. E. Sebastian, V. S. Zapf, N. Harrison, C. D. Batista, P. A. Sharma, M. Jaime, I. R. Fisher and A. Lacerda, *Phys. Rev. Lett.* **96**, 189703 (2006).
- [11] T. Radu, H. Wilhelm, V. Yushankhai, D. Kovrizhin, R. Coldea, Z. Tylczynski, T. Lühmann, and F. Steglich, *Phys. Rev. Lett.* **96**, 189704 (2006).
- [12] V. S. Zapf, D. Zocco, B. R. Hansen, M. Jaime, N. Harrison, C. D. Batista, M. Kenzelmann, C. Niedermayer, A. Lacerda, and A. Paduan-Filho, *Phys. Rev. Lett.* **96**, 077204 (2006).
- [13] D. L. Bergman, R. Shindou, G. A. Fiete, and L. Balents, *Phys. Rev. Lett.* **96**, 097207 (2006).
- [14] A. Kitada, Z. Hiroi, Y. Tsujimoto, T. Kitano, H. Kageyama, Y. Ajiro, and K. Yoshimura, *J. Phys. Soc. Jpn.* **76**, 093706 (2007).
- [15] V. O. Garlea *et al.*, *Phys. Rev. Lett.* **98**, 167202 (2007).
- [16] A. A. Aczel, H. A. Dabkowska, P. R. Provencher, and G. M. Luke, *J. Cryst. Growth* **310**, 870 (2008).
- [17] C. D. Batista and G. Ortiz, *Phys. Rev. Lett.* **86**, 1082 (2001).
- [18] C. D. Batista and G. Ortiz, *Adv. Phys.* **53**, 1 (2004).
- [19] K.-K. Ng and T.-K. Lee, arXiv:cond-mat/0507663.
- [20] H.-T. Wang and Y. Wang, *Phys. Rev. B* **71**, 104429 (2005).
- [21] T. Nikuni, M. Oshikawa, A. Oosawa, and H. Tanaka, *Phys. Rev. Lett.* **84**, 5868 (2000).
- [22] O. Nohadani, S. Wessel, B. Normand, and S. Haas, *Phys. Rev. B* **69**, 220402(R) (2004).
- [23] S. E. Sebastian, P. A. Sharma, M. Jaime, N. Harrison, V. Correa, L. Balicas, N. Kawashima, C. D. Batista, and I. R. Fisher, *Phys. Rev. B* **72**, 100404(R) (2005).
- [24] S. E. Sebastian, N. Harrison, C. D. Batista, L. Balicas, M. Jaime, P. A. Sharma, N. Kawashima, and I. R. Fisher, *Nature (London)* **441**, 617 (2006).
- [25] S. A. Zvyagin, J. Wosnitza, C. D. Batista, M. Tsukamoto, N. Kawashima, J. Krzystek, V. S. Zapf, M. Jaime, N. F. Oliveira Jr., and A. Paduan-Filho, *Phys. Rev. Lett.* **98**, 047205 (2007).
- [26] A. Paduan-Filho, C. D. Batista, P. Sengupta, V. S. Zapf, M. Jaime, A. Lacerda, and K. A. Alhassanieh (to be published).